IEEE Access
Multidisciplinary | Rapid Review | Open Access Journal

Received July 13, 2020, accepted August 3, 2020, date of publication August 13, 2020, date of current version August 25, 2020.

*Digital Object Identifier 10.1109/ACCESS.2020.3016497*

# Development of a Unified Lane-Keeping and Collision Avoidance System for Semi-Trailer Truck

**JUNGGUN YANG[1], SEUNGKI KIM[2], AND KUNSOO HUH[1], (Member, IEEE)**
[1]Department of Automotive Engineering, Hanyang University, Seoul 133-791, South Korea
[2]Research and Development Division, Hyundai Motor Company, Hwaseong 18280, South Korea

Corresponding author: Kunsoo Huh (khuh2@hanyang.ac.kr)

This work was supported by the Ministry of Trade, Industry, and Energy (MOTIE), South Korea, through the Technology Innovation Program (Industrial Strategic Technology Development Program, Development of Automated Driving Systems and Evaluation) under Grant 20006862.

**ABSTRACT** In this article, a unified lane-keeping and forward collision avoidance system is proposed for semi-trailer trucks. Kinematic and dynamic models are described for lateral motion of the semi-trailer truck. The variation of the cornering stiffness is considered because its value depends on driving conditions such as vehicle speed and vertical load. The proposed system consists of the hitch angle estimation algorithm of the semi-trailer truck and the Model Predictive Controller (MPC) for the lateral motion of the semi-trailer truck. In the hitch angle estimation, the disturbance observer is utilized to compensate the lateral uncertainties and the estimation performance is validated in simulations and experiments. In the controller design, an MPC controller is designed both for lane keeping and collision avoidance, but their constraints in lateral motion are considered separately. In constructing the objective functions, constraint smoothing is applied to improve the feasibility of the semi-trailer truck motion. A simplification method is also introduced to reduce the computational complexity of the MPC and to improve the real-time performance. The proposed system is evaluated in simulations for lane keeping and collision avoidance, respectively.

**INDEX TERMS** Autonomous vehicle, semi-trailer truck, model predictive control, collision avoidance system, lane-keeping system.

## I. INTRODUCTION

A semi-trailer truck is the combination of a tractor and semi-trailer unit. This vehicle is widely used in the transportation industry, but it is heavier than passenger vehicle due to heavy weight of tractor and trailer. Because of this feature, the vehicle takes more time to decelerate than passenger vehicle and causes worse fatal consequences in accident. According to Large truck and bus crash facts (LTBCF), which summarizes the traffic incidents in 17 U.S states based on data provided by the National Highway Traffic Safety Administration (NHTSA) between 1975 and 2016, the rate of fatal crashes per 100 million traveled miles of heavy commercial vehicle accidents is greater than the rate of general passenger vehicle [1], [2]. In addition, the rates of fatal crashes involving large trucks per 100 million traveled miles is 1.34 and the rates of fatalities per 100 million traveled miles is 1.50.

According to European accident research and safety report [3], major risk scenarios related to large commercial vehicles can be classified into three types; between commercial vehicles or commercial vehicle alone accidents, commercial vehicle and passenger car accidents, and commercial vehicles and other driving/non-driver accidents. It is also analyzed [3] that Lane keeping assist (LKA) and Lateral collision avoidance assist (LCA) system can avoid accidents in most scenarios. Unlike large commercial vehicles, the Lane keeping assist system has been already commercialized by many automakers for passenger vehicles. In addition, researches on Lateral collision avoidance assistance system for passenger vehicle are getting more attention and some companies are planning to commercialize the assistance system for lateral collision avoidance. In contrast, researches on driver assistance system for semitrailer truck,

The associate editor coordinating the review of this manuscript and approving it for publication was Nabil Benamar.

especially among large commercial vehicles, are insufficient. Although driver assist systems such as Lane Keeping Assist, Lane following assist, and Autonomous emergency braking (AEB) have been commercialized for several large commercial vehicles, researches on collision avoidance through lateral control has not been conducted well in the related community.

In passenger vehicles, various methods have been studied for collision avoidance through steering and additional actuator. He *et al.* [4] evaluated the risk associated with collision by modeling dynamic threat assessment model. Their system includes a path planner based on kinematics and dynamics of vehicle system, that determines a collision-free path when it suddenly encounters emergency scenarios. Taherian *et al.* [5] proposed a collision-free evasive trajectory and a torque vectoring controller based on optimal control to ensure lateral-yaw stabilization. Their system was compared with the system without the torque vectoring and showed that collision avoidance with torque vectoring was effective. Hajiloo *et al.* [6] developed an integrated controller for autonomous vehicles, capable of suitably reacting to emergency situations when a sudden obstacle appears on the road. Model Predictive Control (MPC) was designed for path planning and tracking controller with a hierarchical structure that prioritize collision avoidance, vehicle stability and path tracking by using active front steer and differential braking. However, the above systems cannot be directly applied to semi-trailer trucks mainly because the commercial vehicle shows different behavior due to heavier weight, larger wheel-base and, in particular, articulated tractor/trailer with a hitch angle.

In this article, a unified lane-keeping and collision avoidance system is proposed for semi-trailer truck. The lateral motions of the truck are described based on a kinematic model with a hitch angle and based on a dynamic model with inertial elements, respectively. In the dynamics model, cornering stiffness at each wheel is expressed as a function of vertical load and slip angle, and their identification method is presented to consider their variations. The lateral motion of the semi-trailer is largely dependent on the hitch angle which cannot be easily measured. Thus, to estimate the hitch angle, Kalman filter is designed based on the dynamic model and is combined with the kinematic model for measurement update. After a disturbance observer is added in the hitch angle estimator for the robustness, its estimation performance is validated in simulations and experiments with a test semi-trailer truck. Model predictive controller (MPC) is designed to calculate the desired path and the steering angle, where lateral constraints for lane keeping and collision avoidance are considered separately. In order to reduce the computational burden of the MPC controller, the extended kinematic model with an adaptive gain, constraint smoothing method and model simplification with large prediction interval are suggested. The lane keeping and collision avoidance performance of the proposed system is evaluated in simulations.

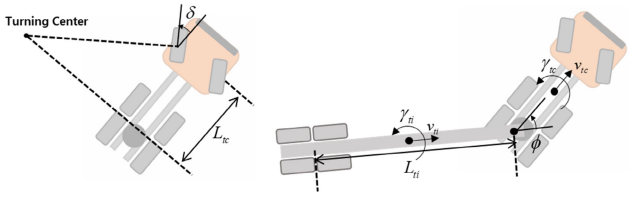


**FIGURE 1.** Geometric relations of semi-trailer truck.

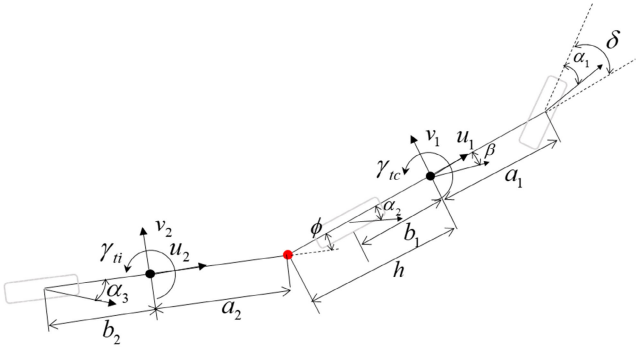


**FIGURE 2.** Bicycle model for semi-trailer truck.

## II. MODELING OF SEMI-TRAILER TRUCK MOTION

In this section, lateral motion of semi-trailer truck is described based on kinematic and dynamic characteristics, respectively. In addition, variation of the cornering stiffness is considered in calculating the lateral tire force.

### A. KINEMATIC MODEL

Figure 1 shows the situation where the semi-trailer truck is turning to the left with road wheel angle $\delta$ at low speed. The slip of each tire is ignored when the vehicle travels at low speed. Under this condition, the yaw rate of the tractor can be obtained in (1) using Ackerman geometry [7]. As shown in the right figure of Figure 1, the hitch angle between the tractor and trailer acts as the steering angle to the trailer and the yawrate of the trailer can be obtained as shown in (2). Using (1)-(2), the hitch angle rate caused by the relative yaw motion of the tractor and trailer can be expressed in (3).

$$\gamma_{tc} = \frac{v_{tc}}{L_{tc}} \tan\delta \tag{1}$$

$$\gamma_{ti} = \frac{v_{ti}}{L_{ti}} \tan\phi \tag{2}$$

$$\begin{aligned} \dot{\phi} &= \gamma_{tc} - \gamma_{ti} \\ &= \frac{v_{tc}}{L_{tc}} \tan\delta - \frac{v_{ti}}{L_{ti}} \tan\phi \\ &= \frac{v_{tc}}{L_{tc}} \tan\delta - \frac{v_{tc}}{L_{ti}} \sin\phi \end{aligned} \tag{3}$$

where

$\gamma_i$ : Yawrate of tractor ($i = tc$) and trailer ($i = ti$)
$L_{tc}$ : Length between front and rear wheels of tractor
$L_{ti}$ : Length between hitch point and rear wheel of trailer
$v_i$ : Longitudinal velocity of tractor ($i = tc$) and trailer ($i = ti$)

### B. DYNAMIC MODEL

Figure 2 shows the free body diagram of the semi-trailer truck by considering tire slip at high speed. The dynamic model is

obtained based on the Lagrange equation for the motion of the semi-trailer truck [8]–[10]. In this model, several assumptions are used. First, small hitch angle and tire slip angle are assumed. Second, the left and right tires on an axle can be lumped into a single equivalent tire. Third, there is little body roll that can affect the lateral motion of semi-trailer truck. With these assumptions, the derived equation of motion is as follows.

$$\begin{aligned}(m_{tc}+m_{ti})(\dot{v}_1+u_1\gamma_{tc})-m_{ti}(h+a_2)\dot{\gamma}_{tc}-m_{ti}a_2\ddot{\phi}\\ =-\frac{1}{u_1}\left[(C_1+C_2)v_1+\{C_{s_1}-C_3(h+a_2+b_2)\}\gamma_{tc}\right.\\ \left.-\ C_3(a_2+b_2)\dot{\phi}\right]+C_1\delta \qquad (4)\\ -hm_{ti}(\dot{v}_1+u_1\gamma_{tc})+\{I_{tc}+m_{ti}h(h+a_2)\}\dot{\gamma}_{tc}+m_{ti}ha_2\ddot{\phi}\\ =-\frac{1}{u_1}\left[C_{s_1}v_1+\{C_{q_1^2}+C_3h(h+a_2+b_2)\}\gamma_{tc}\right.\\ \left.+\ C_3h(a_2+b_2)\dot{\phi}\right]+C_1a_1\delta \qquad (5)\\ -m_{ti}a_2\left(\dot{v}_1+u_1\gamma_{tc}\right)+\left\{I_{ti}+m_{ti}a_2\left(h+a_2\right)\right\}\dot{\gamma}_{tc}\\ +\left(I_{ti}+m_{ti}a_2^2\right)\ddot{\phi}\\ =-\frac{C_3(a_2+b_2)}{u_1}\left[-v_{tc}+\left(h+a_2+b_2\right)\gamma_{tc}\right.\\ \left.+\ \left(a_2+b_2\right)\left(\dot{\phi}+u_{tc}\phi\right)\right] \qquad (6)\end{aligned}$$

where

$C_i$ : cornering stiffness of front tires ($i=1$) and rear tires ($i=2$) of tractor

$C_3$ : cornering stiffness of trailer tires

$$C_{s1}=a_1C_1-b_1C_2$$
$$C_{q_1^2}=a_1^2C_1+b_1^2C_2$$

$u_1, v_1$ : longitudinal and lateral velocity of tractor

$u_2, v_2$ : longitudinal and lateral velocity of trailer

$m_i$ : mass of tractor ($i=tc$) and trailer ($i=ti$)

$I_i$ : moment of inertia of tractor ($i=tc$) and trailer ($i=ti$)

The cornering stiffness depends on the slip angle and its effect is considered in this study. Equation (4∼6) can be expressed in the following state-space equation form.

$$\dot{X}=M^{-1}A.X+M^{-1}B.U \qquad (7)$$

where, $X$, $M$, $A$, and $B$, as shown at the bottom of the next page. Or, in discrete form:

$$X_{k+1}=A_dX_k+B_dU_k \qquad (8)$$

where $A_d=(I+M^{-1}A\Delta t)$, $B_d=M^{-1}B\Delta t$

$\Delta t$ is the sampling time in discretization. The derived state-space equation is used for the hitch angle estimator design for semi-trailer truck.

### C. CORNERING STIFFNESS MODELING

The lateral tire force can be expressed with the cornering stiffness and the slip angle of the tire. Generally, constant cornering stiffness is obtained by the slope of the linear part in the low-slip region. Because the value of the cornering stiffness depends on the driving condition such as speed and vertical load, its variation needs to be considered. Figure 3 shows the tire model provided by the TruckSim [11] where the lateral tire force is plotted with different vertical force and slip angle.

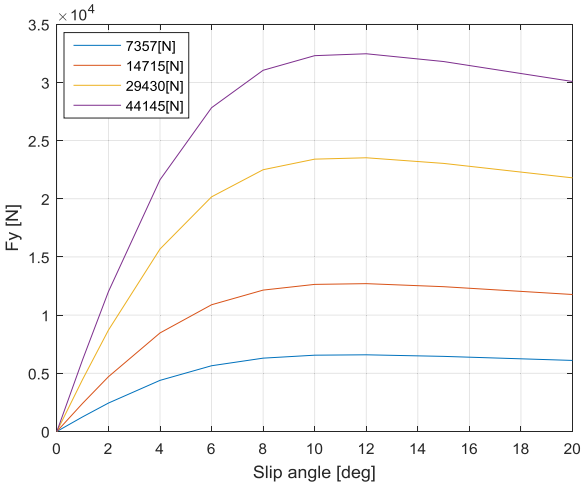


**FIGURE 3.** Lateral tire force w.r.t. slip angle (commercial vehicle).

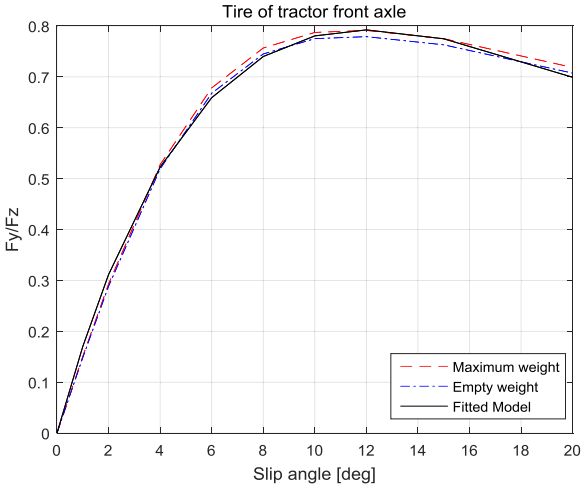


**FIGURE 4.** Lateral force divided by vertical load and fitted model.

In this study, an exponential tire model is suggested such that it can be applied even in situations of empty weight and maximum weight. First, the lateral force, $F_y$, at each tire is assumed as (9) and is divided by the corresponding vertical force, $F_z$. The upper and lower bounds of the ratio ($F_y/F_z$) are obtained for empty weight and maximum weight of the trailer. The range of bounds is small as shown in Figure 4 for all tires at tractor front, tractor rear and trailer axles. The ratio at each axle is fitted into (9) and its parameters are determined. As a result, the cornering stiffness, $C_i$, that is variable to slip angle and vertical load can be obtained as (10).

$$F_{y_i}=F_{z_i}(P_1\exp(P_2\cdot\alpha_i+P_3))\cdot\alpha_i \qquad (9)$$
$$C_i=F_{z_i}(P_1\exp(P_2\cdot\alpha_i+P_3)) \qquad (10)$$

where $P_i$ is a fitting parameter for the exponential function

## III. ESTIMATION OF THE HITCH ANGLE

In a semi-trailer truck, hitch angle occurs due to the relative yaw motion between the tractor and trailer. The hitch angle is the factor that determines the path of the trailer and its information is necessary in predicting the lateral behavior of the trailer. Because the hitch angle cannot be easily measured, its estimator is designed to describe the lateral motion of the trailer better. In addition, disturbance to the lateral motion is estimated to minimize the effects of the unintended lateral force such as road grade, lateral wind, etc.

### A. HITCH ANGLE ESTIMATOR DESIGN

Since typical semi-trailer truck does not have a hitch angle sensor, it is necessary to estimate the hitch angle. In the case of low-speed driving, tire slip angle is small and the kinematic model derived in (3) can represent the hitch angle properly even if the hitch angle becomes large. However, in high-speed cases, due to the existence of tire slip, the kinematic model in (3) is not valid anymore. On the other hand, the dynamic model in (8) can be utilized to estimate the hitch angle by assuming that the hitch angle is small and approximated. It should be noted that estimation error in the hitch angle can cause problems in the prediction and control of the semi-trailer truck. Therefore, in this study, an integrated estimation method is proposed using a combination of dynamic model (8) and kinematic model (3). First, the Kalman filter [12] is designed based on the dynamic model (8) as follows:

$$\begin{aligned}
\hat{X}_k^- &= A_d \hat{X}_{k-1} + B_d U_{k-1} \\
P_k^- &= A_d P_{k-1} A_d^T + Q \\
K_k &= P_k^- H^T (H P_k^- H^T + R)^{-1} \\
\hat{X}_k &= \hat{X}_k^- + K_k (y_k - H \hat{X}_k^-) \\
P_k &= P_k^- - K_k H P_k^-
\end{aligned} \tag{11}$$

Secondly, to improve the performance of the Kalman filter, the hitch angle calculated from the kinematic model (3) is used as a measurement value. The structure of the proposed estimator is shown in Figure 5.

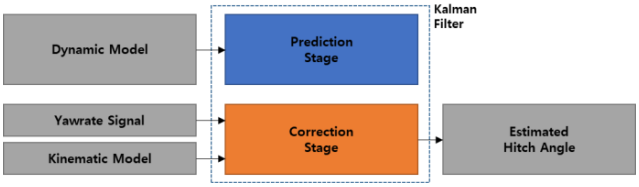


**FIGURE 5.** Structure of the proposed estimator.

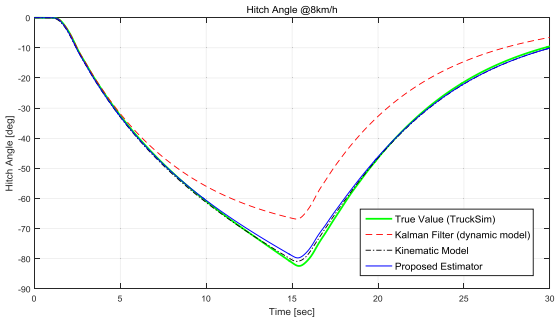


**FIGURE 6.** Simulation result of hitch angle estimation (low speed).

In order to compare the performance of the proposed estimator which integrates the Kalman filter with the kinematic model, simulation is conducted using commercial software of MATLAB/Simulink and TruckSim. Figure 6 shows the simulation results based on the kinematic model only, Kalman filter with the dynamic model only and the proposed estimator. In the first scenario, the speed is 8km/h and the steering input is 550deg maximum. The Kalman filter based on the dynamic model only shows large estimation error. This is due to the small angle assumption on the hitch angle in the dynamic model (8). On the other hand, the hitch angle calculated from the kinematic model (3) is very close to true value. The proposed estimator also shows little error mainly because the kinematic model output is used as a measurement value for the Kalman filter.

$$X = \begin{bmatrix} v_1 & \gamma_{tc} & \dot{\phi} & \phi \end{bmatrix}^T, U = \delta$$

$$M = \begin{bmatrix} m_{tc} + m_{ti} & -m_{ti}(h + a_2) & -m_{ti}a_2 & 0 \\ -m_{ti}h & I_{tc} + m_{ti}h(h + a_2) & m_{ti}ha_2 & 0 \\ -m_{ti}a_2 & I_{ti} + m_2 a_2 (h + a_2) & I_{ti} + m_{ti}a_2^2 & 0 \\ 0 & 0 & 0 & 1 \end{bmatrix}$$

$$A = -\frac{1}{u_1} \begin{bmatrix} C_1 + C_2 + C_3 & C_{S_1} - C_3(h + a_2 + b_2) + (m_{tc} + m_{ti})u_1^2 & -C_3(a_2 + b_2) & -C_3 u_1 \\ C_{s_1} - C_3 h & C_{q_1^2} + C_3 h(h + a_2 + b_2) - m_{ti}hu_1^2 & C_3 h(a_2 + b_2) & C_3 h u_1 \\ -C_3(a_2 + b_2) & C_3(a_2 + b_2)(h + a_2 + b_2) - m_{ti}a_2 u_1^2 & C_3(a_2 + b_2)^2 & C_3(a_2 + b_2)u_1 \\ 0 & 0 & -u_1 & 0 \end{bmatrix}$$

$$B = \begin{bmatrix} C_1 \\ a_1 C_1 \\ 0 \\ 0 \end{bmatrix}$$

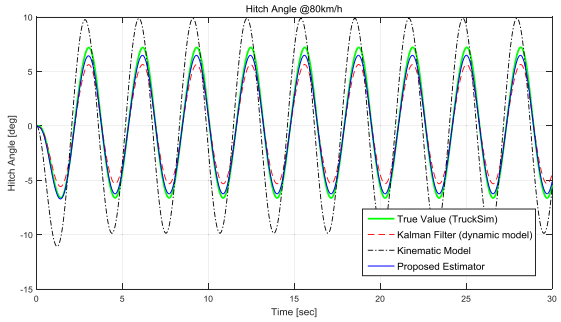


**FIGURE 7.** Simulation result of hitch angle estimation (high speed).

The second scenario is a high-speed 80km/h, ±120deg sine wave steering input situation (Figure 7). Contrary to the first scenario, the Kalman filter based on the dynamic model only shows better accuracy than the kinematic model output. At high speed, there occurs lateral slip on the tire motion and, thus, the kinematic model is not valid anymore. However, the proposed estimator provides accurate estimation of the hitch angle regardless of speed and steering angle.

### B. DISTURBANCE OBSERVER DESIGN

Unintended lateral force can be generated due to road grade and lateral wind. In addition, modeling error can exist in Equation (8). These factors can induce inaccurate hitch angle estimation and its cause is expressed as the disturbance input to the model. From this perspective, the robustness of the hitch angle estimator can be improved through the design of the disturbance observer [13]. To estimate the disturbance, state argumentation is introduced to include the existing states of Equation (8) and the disturbance input. The state space equation with the state argumentation is derived from Equation (8) and is shown below. The Kalman filter is designed based on Equation (11) to estimate the disturbance, $d_k$, and its value is reflected in the hitch angle estimation in Equation (12)

$$\begin{bmatrix} X_{k+1} \\ d_{k+1} \end{bmatrix} = \begin{bmatrix} A_d & B_d \\ 0 & I \end{bmatrix} \begin{bmatrix} X_k \\ d_k \end{bmatrix} + \begin{bmatrix} B_d \\ 0 \end{bmatrix} U_k + \begin{bmatrix} 0 \\ I \end{bmatrix} w_k$$
$$y_k = \begin{bmatrix} C & 0 \end{bmatrix} \begin{bmatrix} X_k \\ d_k \end{bmatrix} + v_k \tag{12}$$

where

$d_k$ : input disturbance
$w_k$ : process noise
$v_k$ : measurement noise

The derived state space equation is used for disturbance observer design.

### C. VALIDATION OF THE ESTIMATOR

#### 1) SIMULATION

This section shows the simulation results of the designed estimator where lateral motion of semi-trailer truck is described by TruckSim [11]. Figure 8 is the simulation result of the hitch angle estimation when the steering input of the sine wave is applied while accelerating from 8 km/h. The proposed estimator with the disturbance observer shows the improved estimation performance both at high and low speed maneuvering.

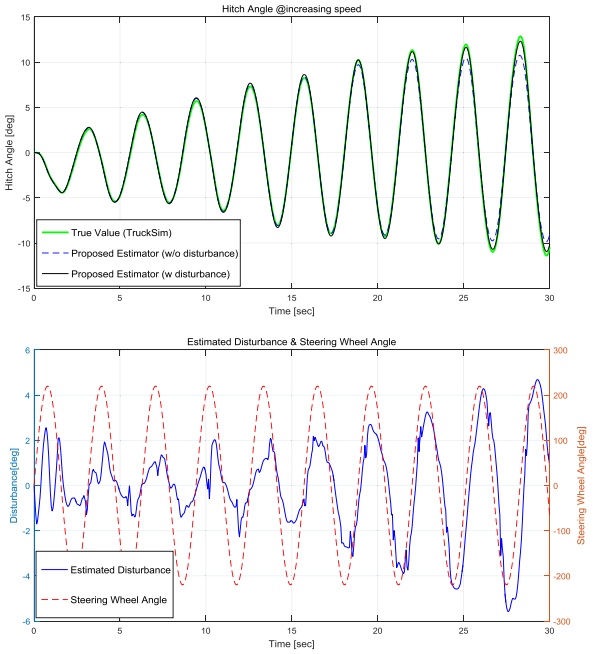


**FIGURE 8.** Simulation result of hitch angle estimation at increasing speed.

#### 2) EXPERIMENTAL TEST

The estimator designed in this article is also verified experimentally by using a 4 × 2 tractor-trailer. The hitch angle is estimated based on the real data and is compared with true value which is measured from the temporarily mounted sensor. The experimental results in Figure 9 demonstrate that the proposed estimator with the disturbance observer provides accurate estimation of the hitch angle not only in small values, but also in large values up to 40 degrees.

## IV. CONTROLLER DESIGN

This section describes lane-keeping control and collision avoidance control of the semi-trailer truck. The proposed steering control algorithm is designed using the Model Predictive Control theory [14] to consider the non-holonomic motion of the tractor and trailer. The kinematic model is utilized in the controller design, and the modeling error at high speed is compensated. In addition, for the robustness, controller is designed to calculate the steering angle that does not diverge even in the presence of an infeasible constraint.

### A. EXTENDED LATERAL KINEMATIC MODEL OF THE ARTICULATED VEHICLE

In order to reduce the computational complexity, controller is designed based on a kinematic model rather than a dynamic model. However, as mentioned in Section 2, the accuracy of the kinematic model is reduced as the slip angle of the

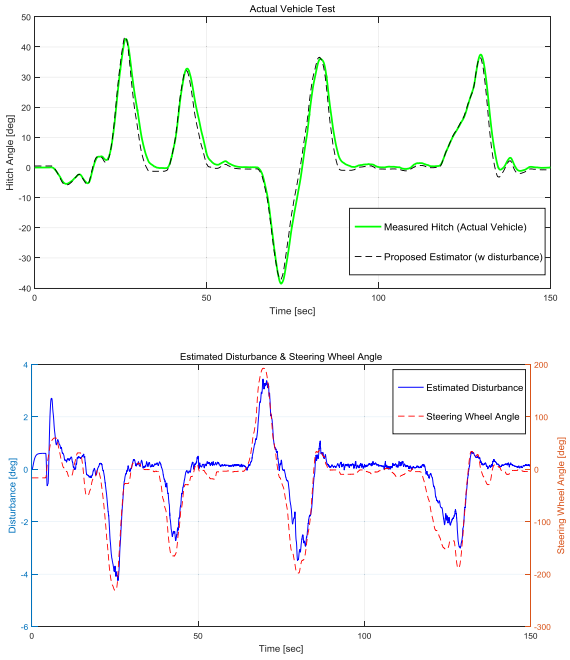


**FIGURE 9.** Experimental test result of hitch angle estimation.

tire increases at high-speed. This limitation is overcome by suggesting a modified kinematic model where an adaptive gain parameter is introduced. Equation (1) is modified as below so that the modified model can be used even at high speed.

$$\gamma_{tc,Model} = L_{gain} \cdot \frac{v_{tc}}{L_{tc}} \tan\delta \tag{13}$$

where

$$L_{gain} = L_{gain,ini} + K_L \cdot \int_0^t (\gamma_{tc,sensor} - \gamma_{tc,Model})dt \tag{14}$$

$L_{gain,ini}$ and $K_L$ are initial gain value and tuning factor, respectively.

The proposed model in Equation (13) does not contain enough information to control the lateral motion such as lateral position and heading angle. Thus, for the lateral control of the semi-trailer truck, an extended model is used with including the lateral position and the heading angle of the tractor. When the semi-trailer truck is turning, the change of the heading angle of the tractor is defined as the yawrate.

$$\dot{\psi}_{tc} = \gamma_{tc} \tag{15}$$

In addition, the lateral velocity of the tractor can be approximated for small $\psi_{tc}$ as follows.

$$\dot{y}_{tc} = v_{tc} \sin(\psi_{tc}) \cong v_{tc}\psi_{tc} \tag{16}$$

By combining the above Equations (13)∼(16), an extended model for semi-trailer truck motion is derived. The steering angle and the hitch angle are small in normal driving of semi-trailer truck and, thus, Equation (3) and (12) can be expressed in linear discrete equations.

$$x^e_{k+1} = A^e x^e_k + B^e u_k \tag{17}$$

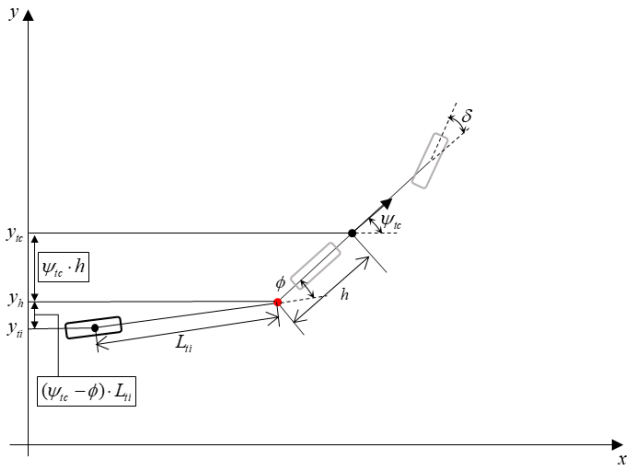


**FIGURE 10.** Lateral position of tractor and trailer.

where

$$A^e = \begin{bmatrix} 1 & dt \cdot v_{tc} & 0 \\ 0 & 1 & 0 \\ 0 & 0 & 1 - dt \cdot \dfrac{v_{tc}}{L_{ti}} \end{bmatrix},$$

$$B^e = L_{gain} \begin{bmatrix} 0 \\ \dfrac{dt \cdot v_{tc}}{L_{tc}} \\ \dfrac{dt \cdot v_{tc}}{L_{tc}} \end{bmatrix}, \; x^e_k = \begin{bmatrix} y_{tc} \\ \psi_{tc} \\ \phi \end{bmatrix}_k, \; u_k = \delta$$

In the above Equation, the hitch angle estimated in Section III is utilized as a state variable. For lane keeping control and collision avoidance control of the semi-trailer truck, it is necessary to consider not only the tractor behavior, but also the position of the semi-trailer. As shown in Figure 10, the lateral position of the semi-trailer can be expressed by using the lateral position of the tractor and small hitch angle.

$$y_{ti} = y_{tc} - (h + L_{ti}) \cdot \psi_{tc} + L_{ti} \cdot \phi \tag{18}$$

Finally, the lateral positions of tractor mass center and the semi-trailer axle, and the heading angle of the tractor are defined as the output variables of the extended model of the semi-trailer truck.

$$Y = H^e x^e_k \tag{19}$$

where

$$Y = \begin{bmatrix} y_{tc} \\ y_{ti} \\ \psi_{tc} \end{bmatrix}, H^e = \begin{bmatrix} 1 & 0 & 0 \\ 1 & -(h + L_{ti}) & L_{ti} \\ 0 & 1 & 0 \end{bmatrix}$$

### B. OUTPUT PREDICTION WITH THE EXTENDED MODEL

For the controller design, Equation (17) is modified to the incremental state space equation where the rate of change of the steering angle is included.

$$\overline{X}^e_{k+1} = \overline{A}\,\overline{X}^e_k + \overline{B}\Delta u_k$$

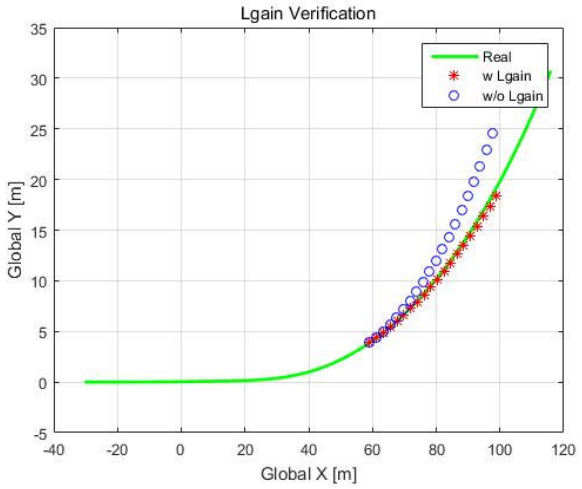


**FIGURE 11.** Prediction result with $L_{gain}$.

$$\overline{Y}_k^e = \overline{H}^e \overline{X}_k^e \tag{20}$$

where

$$\overline{X}_k^e = \begin{bmatrix} x_k^e \\ u_{k-1} \end{bmatrix}, \overline{A} = \begin{bmatrix} A^e & B^e \\ 0 & I \end{bmatrix}, \overline{B} = \begin{bmatrix} B^e \\ I \end{bmatrix}, \overline{H} = \begin{bmatrix} H^e \\ 0 \end{bmatrix}$$

Using the above state-space equation, the output of the k+1th step is predicted as follows.

$$\begin{aligned} \overline{X}_{k+1}^e &= \overline{A} \cdot \overline{X}_k^e + \overline{B} \cdot \Delta u_k \\ \overline{Y}_k^e &= \overline{H} \cdot \overline{X}_{k+1}^e \\ &= \overline{H} \cdot (\overline{A} \cdot \overline{X}_k^e + \overline{B} \cdot \Delta u_k) \\ &= \overline{HA} \cdot \overline{X}_k^e + \overline{HB} \cdot \Delta u_k \end{aligned} \tag{21}$$

Then, the $(k+N)^{th}$ predicted output can be expressed by the following Equation (22).

$$\begin{bmatrix} y_{k+1}^e \\ y_{k+2}^e \\ \vdots \\ y_{k+N}^e \end{bmatrix} = \begin{bmatrix} \overline{HA} \\ \overline{H}(\overline{A})^2 \\ \vdots \\ \overline{H}(\overline{A})^N \end{bmatrix} \overline{X}_k^e + \begin{bmatrix} \overline{HB} & 0 & \cdots & 0 \\ \overline{HAB} + \overline{HB} & \overline{HB} & \cdots & 0 \\ \vdots & \vdots & & \\ \sum_i^N \overline{H}(\overline{A})^{i-1}\overline{B} & \sum_i^{N-1} \overline{H}(\overline{A})^{i-1}\overline{B} & \cdots & \end{bmatrix} \times \begin{bmatrix} \Delta u_k \\ \Delta u_{k+1} \\ \vdots \\ \Delta u_{k+N-1} \end{bmatrix} \tag{22}$$

### C. VERIFICATION OF OUTPUT PREDICTION

To evaluate the performance of the prediction model, simulation is performed via MATLAB/Simulink and TruckSim. Figure 11 shows the output prediction results of a scenario where 75deg step steering wheel input is applied with the vehicle speed of 80km/h. The prediction horizon is 2 seconds with the time step of 0.01 seconds. Green line is the actual trajectory of Semi-tractor trailer obtained by TruckSim, while blue circle and red asterisk lines represent the prediction results without and with the adaptive gain, $L_{gain}$, respectively. The prediction results clearly demonstrate the effect of the adaptive gain in the vehicle model, which will be used in the MPC controller design.

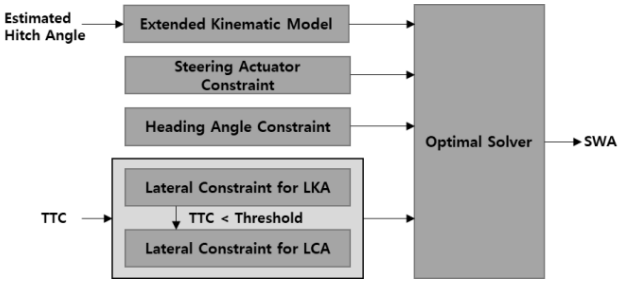


**FIGURE 12.** Structure of steering control algorithm.

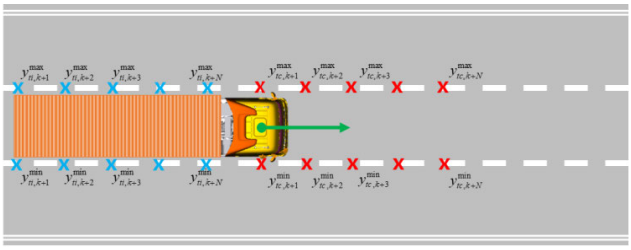

**FIGURE 13.** Lateral constraint for lane keeping assistant (Straight road).

### D. STEERING CONTROL ALGORITHM DESIGN BASED ON MODEL PREDICTIVE CONTROL

The steering control algorithm proposed in this study calculates the optimized steering angle under the heading angle, steering actuator and lateral constraint. This algorithm is a combined system of lane keeping and collision avoidance system. Therefore, method to combine these two systems is necessary. In this study, when there is no risk of collision, the lateral constraint for lane keeping control is used basically. When there is a risk of collision (when TTC is smaller than threshold) the lateral constraint is turns into a collision avoidance case. The overall control algorithm structure is shown in Figure 12.

#### 1) LATERAL CONSTRAINT FOR LANE KEEPING

Figure 13 shows the boundary of the lane in which the semi-trailer truck is driving on straight road. In order to pass through the drivable space without lane departure, lateral positions of both tractor and the semi-trailer must be inside the boundary. The lateral boundary constraints of the drivable space at each step can be expressed in the form of constraint vectors.

$$\begin{aligned} \boldsymbol{y}_{tc,k}^{\min} &\le \boldsymbol{y}_{tc,k} \le \boldsymbol{y}_{tc,k}^{\max} \\ \boldsymbol{y}_{ti,k}^{\min} &\le \boldsymbol{y}_{ti,k} \le \boldsymbol{y}_{ti,k}^{\max} \end{aligned} \tag{23}$$

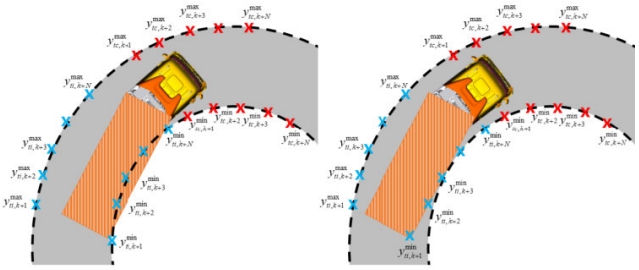


**FIGURE 14.** Lateral constraint for lane keeping assistant (Curved road).

where

$$\begin{aligned}
\boldsymbol{y}_{tc,k} &= \begin{bmatrix} y_{tc,k+1} & y_{tc,k+2} & \cdots & y_{tc,k+N} \end{bmatrix}^T \\
\boldsymbol{y}_{ti,k} &= \begin{bmatrix} y_{ti,k+1} & y_{ti,k+2} & \cdots & y_{ti,k+N} \end{bmatrix}^T \\
\boldsymbol{y}^{\min}_{tc,k} &= \begin{bmatrix} y^{\min}_{tc,k+1} & y^{\min}_{tc,k+2} & \cdots & y^{\min}_{tc,k+N} \end{bmatrix}^T \\
\boldsymbol{y}^{\max}_{tc,k} &= \begin{bmatrix} y^{\max}_{tc,k+1} & y^{\max}_{tc,k+2} & \cdots & y^{\max}_{tc,k+N} \end{bmatrix}^T \\
\boldsymbol{y}^{\min}_{ti,k} &= \begin{bmatrix} y^{\min}_{ti,k+1} & y^{\min}_{ti,k+2} & \cdots & y^{\min}_{ti,k+N} \end{bmatrix}^T \\
\boldsymbol{y}^{\max}_{ti,k} &= \begin{bmatrix} y^{\max}_{ti,k+1} & y^{\max}_{ti,k+2} & \cdots & y^{\max}_{ti,k+N} \end{bmatrix}^T
\end{aligned}$$

However, when the semi-trailer truck drives on a curved road, the side wall of the trailer can deviate from the lane boundary due to the long length of trailer. Therefore, the lateral constraint of semi-trailer axle should be modified to prevent both axle and side wall of the trailer from lane departure. To obtain the modified lateral constraint, the predicted hitch angle obtained by the previously designed model (22) and the curvature of lane boundary is used. Figure 14 shows the concept of the modified constraint.

### 2) LATERAL CONSTRAINT FOR COLLISION AVOIDANCE

The collision avoidance system needs to predict the situation in advance and act to prevent collisions through proper control input. Figure 15 shows the boundaries of drivable space in two situations. Even if the obstacle is located in front of the ego vehicle, it is not appropriate to judge this obstacle dangerous when the speed of the obstacle vehicle is faster or the TTC(Time to Collision) of the target vehicle is larger than the threshold value.

In the top plot of Figure 15, since the TTC of the obstacle vehicle is larger than threshold, it is shown that the lateral constraint is the ego lane itself. However, in Figure 16, collision inside the ego lane is expected based on the predicted path of the ego vehicle and, thus, the lateral constraint is set to the next lane to avoid the collision

Figure 16 shows a scenario where the obstacle vehicle cuts in front of the semi-trailer truck from the left lane. The obstacle position is predicted with a constant velocity (CV) model [15] to judge collision and the lateral constraint is extended to the next lane.

### 3) HEADING ANGLE CONSTRAINT

In semi-trailer trucks, the height of vehicle center of gravity (CG) is higher than passenger cars and roll-over can be caused

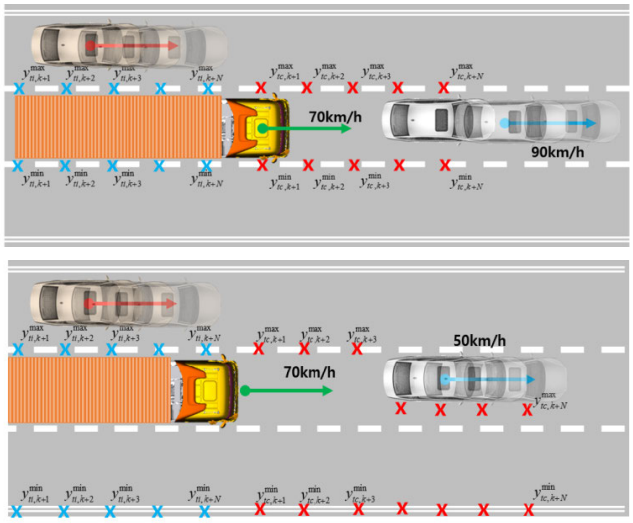


**FIGURE 15.** Lateral constraint for collision avoidance.

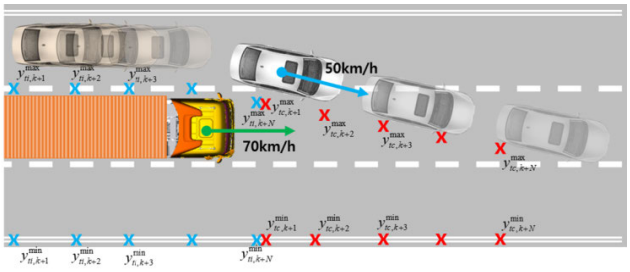


**FIGURE 16.** Lateral constraint for collision avoidance (Cut-in Scenario).

easily during abrupt steering input. For example, the lateral acceleration is used as an index of roll-over [16]. In this study the lateral acceleration is approximated as follows when the semi-trailer truck is turning slowly.

$$a_y = v_y + v_x \cdot \gamma \approx v_x \cdot \gamma \tag{24}$$

Since the output variable of the extended articulated vehicle model in (19) does not include this variable, heading angle of semi-trailer can be utilized to describe the yawrate.

$$\mathbf{r}_k = H\Psi_k \tag{25}$$

where

$$\begin{aligned}
\boldsymbol{\Psi}_k &= \begin{bmatrix} \Psi_{k+1} & \Psi_{k+2} & \cdots & \Psi_{k+N} \end{bmatrix}^T \\
\mathbf{r}_k &= \begin{bmatrix} \gamma_{k+1} & \gamma_{k+1} & \cdots & \gamma_{k+N} \end{bmatrix}^T \\
H &= \frac{1}{dt}\begin{bmatrix} -1 & 1 & 0 & \cdots & 0 \\ 0 & -1 & 1 & \cdots & 0 \\ 0 & 0 & -1 & \cdots & 0 \\ \vdots & \vdots & \vdots & \ddots & 0 \\ 0 & 0 & 0 & -1 & 1 \end{bmatrix}
\end{aligned}$$

Thus, the constraint for the yawrate can be considered in the heading angle as follows:

$$H^{-1}\mathbf{r}_k^{\min} \le \Psi_k \le H^{-1}\mathbf{r}_k^{\max} \tag{26}$$

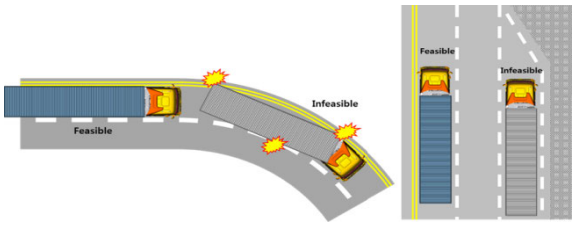


**FIGURE 17.** Cases of infeasible constraint set.

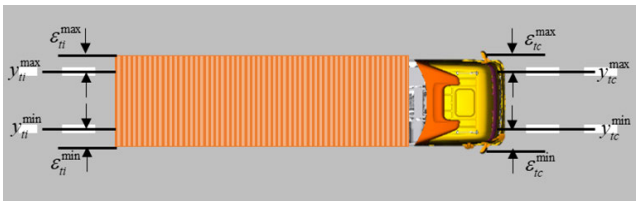

**FIGURE 18.** Slack variable for infeasible constraint set.

where

$$\mathbf{r}_k^{\max} = \frac{1}{v_x}\begin{bmatrix} a_{y,k+1}^{\max} & a_{y,k+2}^{\max} & \cdots & a_{y,k+N}^{\max} \end{bmatrix}^T$$
$$\mathbf{r}_k^{\min} = \frac{1}{v_x}\begin{bmatrix} a_{y,k+1}^{\min} & a_{y,k+2}^{\min} & \cdots & a_{y,k+N}^{\min} \end{bmatrix}^T$$

#### 4) STEERING ACTUATOR CONSTRAINT

The maximum steering angle of the vehicle is physically limited. In addition, the maximum steering speed is also limited by the actuator capacity for steering control. In this study, the following constraints are formulated to consider the physical limits of the steering actuator.

$$\begin{aligned} \mathbf{u}_k^{\min} &\le \mathbf{u}_k \le \mathbf{u}_k^{\max} \\ \Delta\mathbf{u}_k^{\min} &\le \Delta\mathbf{u}_k \le \Delta\mathbf{u}_k^{\max} \end{aligned} \tag{27}$$

where

$$\begin{aligned} \mathbf{u}_k &= \begin{bmatrix} \delta_{k+1} & \delta_{k+2} & \cdots & \delta_{k+N} \end{bmatrix} \\ \mathbf{u}_k^{\min} &= \begin{bmatrix} \delta_{k+1}^{\min} & \delta_{k+2}^{\min} & \cdots & \delta_{k+N}^{\min} \end{bmatrix} \\ \mathbf{u}_k^{\max} &= \begin{bmatrix} \delta_{k+1}^{\max} & \delta_{k+2}^{\max} & \cdots & \delta_{k+N}^{\max} \end{bmatrix} \\ \Delta\mathbf{u}_k &= \begin{bmatrix} \Delta\delta_{k+1} & \Delta\delta_{k+2} & \cdots & \Delta\delta_{k+N} \end{bmatrix} \\ \Delta\mathbf{u}_k^{\min} &= \begin{bmatrix} \Delta\delta_{k+1}^{\min} & \Delta\delta_{k+2}^{\min} & \cdots & \Delta\delta_{k+N}^{\min} \end{bmatrix} \\ \Delta\mathbf{u}_k^{\max} &= \begin{bmatrix} \Delta\delta_{k+1}^{\max} & \Delta\delta_{k+2}^{\max} & \cdots & \Delta\delta_{k+N}^{\max} \end{bmatrix} \end{aligned}$$

#### 5) OBJECTIVE FUNCTION DESCRIPTION

The proposed system operates in hazardous situations where lane departure or forward collision is expected. Therefore, in this study, the following object function is defined not only to avoid the risky situation, but also to minimize the steering control intervention when no risk occurs.

$$J = \left(\mathbf{y}^e\right)^T Q_{\mathbf{w}} \mathbf{y}^e + \Delta\mathbf{u}^T Q_{\mathbf{u}} \Delta\mathbf{u} \tag{28}$$

where $\boldsymbol{y}^e = \begin{bmatrix} y_{tc} & y_{ti} & \psi_{tc} \end{bmatrix}^T$. $Q_{\boldsymbol{w}}$ and $Q_{\boldsymbol{u}}$ are weight matrices for lateral performance and control input, respectively

### E. CONSTRAINT SMOOTHING FOR ROBUSTNESS

In this optimization problem, if there is an infeasible constraint set, such as when the left/right boundary is narrower than the vehicle width of the semi-trailer truck, the optimal solution cannot be obtained or diverge. Figure 17 shows an example of an infeasible constraint set that can be encountered in driving.

The lateral position constraint of Equation (23) is rewritten in Equation (29) such that the suboptimal control input can be calculated stably even in the presence of infeasible constraint sets.

$$\begin{aligned} \boldsymbol{y}_{tc,k}^{\min} - \varepsilon_{tc}^{\min} &\le \boldsymbol{y}_{tc,k} \le \boldsymbol{y}_{tc,k}^{\max} + \varepsilon_{tc}^{\max} \\ \boldsymbol{y}_{ti,k}^{\min} - \varepsilon_{ti}^{\min} &\le \boldsymbol{y}_{ti,k} \le \boldsymbol{y}_{ti,k}^{\max} + \varepsilon_{ti}^{\max} \end{aligned} \tag{29}$$

where $\varepsilon \ge 0$

In Equation (29), $\varepsilon$ is a slack variable to mitigate the constraints on the left and right boundaries of the tractor and semi-trailer [17], [18]. Figure 18 illustrates the role of slack variable, $\varepsilon$, in infeasible constraint sets.

If the size of the slack variable, $\varepsilon$, becomes very large, it is impossible to prevent a lane departure of the vehicle or a collision with the adjacent vehicles. The objective function of Equation (28) is modified as follows to minimize the size of the slack variable.

$$J = \left(\mathbf{y}^e\right)^T Q_{\mathbf{w}} \mathbf{y}^e + \Delta\mathbf{u}^T Q_{\mathbf{u}} \Delta\mathbf{u} + \mathbf{e}^T Q_{\varepsilon} \mathbf{e} \tag{30}$$

where $\mathbf{e} = \begin{bmatrix} \varepsilon_{tc}^{\max} & \varepsilon_{tc}^{\min} & \varepsilon_{ti}^{\max} & \varepsilon_{ti}^{\min} \end{bmatrix}^T$ and $Q_{\varepsilon}$ is the weight matrix for the slack variables.

### F. METHOD FOR REDUCING THE COMPUTATIONAL COMPLEXITY OF MPC

Model Predictive Controller finds the optimal solution created by accumulating the predicted outputs of the state space equations. Therefore, the computational complexity is much larger than non-predictive controllers, and it is greatly influenced by the size of the stacked matrix. In order to overcome these limitations, a simplification method is suggested to reduce the stacked matrix size of MPC.

There are two approaches to reduce the stacked matrix size; by decreasing the model order or the number of states and by increasing the prediction sample time. The first approach is realized in this study by using the kinematic model instead of the dynamic model, and the second approach is also considered here. For the conventional MPC, the optimal solution is calculated by matching the MPC prediction cycle with the discretization sampling time of the state space equation.

If the discretization sampling time is increased to reduce the computational complexity, the accuracy of the model will be reduced as illustrated in Figure 19

To overcome this problem, it is suggested to increase the MPC prediction cycle while maintaining the discretization sampling time of the state space equation. For the implementation of this method, input of the discretized model is assumed constant until the next prediction step. Figure 20 shows the concept of the proposed method.

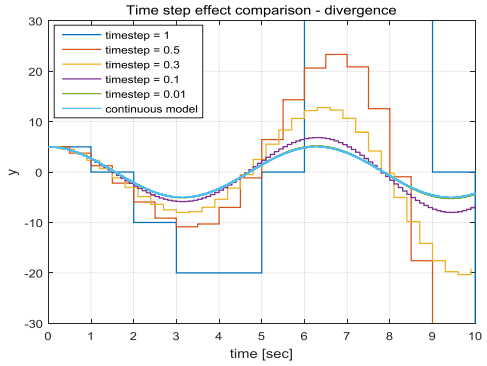


**FIGURE 19.** Model difference with various discretized sampling time.

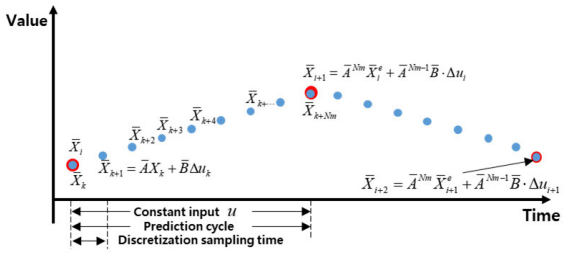


**FIGURE 20.** Concept of the proposed simplification method.

The modified model created by this approach is obtained assuming that the value at the Initial step of discretization and prediction are same.

$$\overline{X}_k = \overline{X}_i$$

where $k$ and $i$ are discretization and prediction steps, respectively.

Then, to reduce computation complexity, input of the discretized model is maintained constant until the next prediction cycle ($\Delta u_{k+1} \sim \Delta u_{k+Nm} = 0$). Using this condition, the following equation can be derived.

$$\begin{aligned}
\overline{X}_{k+1} &= \overline{A}\,\overline{X}_k + \overline{B}\cdot\Delta u_k \\
\overline{X}_{k+2} &= \overline{A}\,\overline{X}_{k+1} + \overline{B}\cdot\Delta u_{k+1} \\
&= \overline{A}\left(\overline{A}\,\overline{X}_k + \overline{B}\cdot\Delta u_k\right) + \overline{B}\cdot\Delta u_{k+1} \\
&= \overline{A}^2\,\overline{X}_k + \overline{A}\,\overline{B}\cdot\Delta u_k \\
\overline{X}_{k+3} &= \overline{A}\,\overline{X}_{k+2} + \overline{B}\cdot\Delta u_{k+2} \\
&= \overline{A}\left(\overline{A}^2\overline{X}_k + \overline{A}\,\overline{B}\cdot\Delta u_k\right) + \overline{B}\cdot\Delta u_{k+2} \\
&= \overline{A}^3\,\overline{X}_k + \overline{A}^2\overline{B}\cdot\Delta u_k \\
&\vdots \\
\overline{X}^e_{k+Nm-1} &= \overline{A}^{Nm-1}\overline{X}^e_k + \overline{A}^{Nm-2}\overline{B}\cdot\Delta u_k \\
\overline{X}_{k+Nm} &= \overline{A}^{Nm}\overline{X}^e_k + \overline{A}^{Nm-1}\overline{B}\cdot\Delta u_k = \overline{X}_{i+1} \\
&= \overline{A}^{Nm}\overline{X}_i + \overline{A}^{Nm-1}\overline{B}\cdot\Delta u_i
\end{aligned} \tag{31}$$

Figure 21 shows the result of the computation time and this method can reduce the computation time greatly compare to conventional MPC.

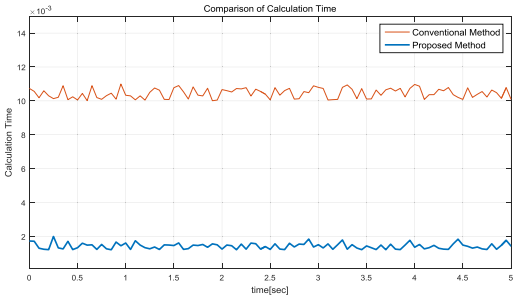


**FIGURE 21.** Result of computation time.

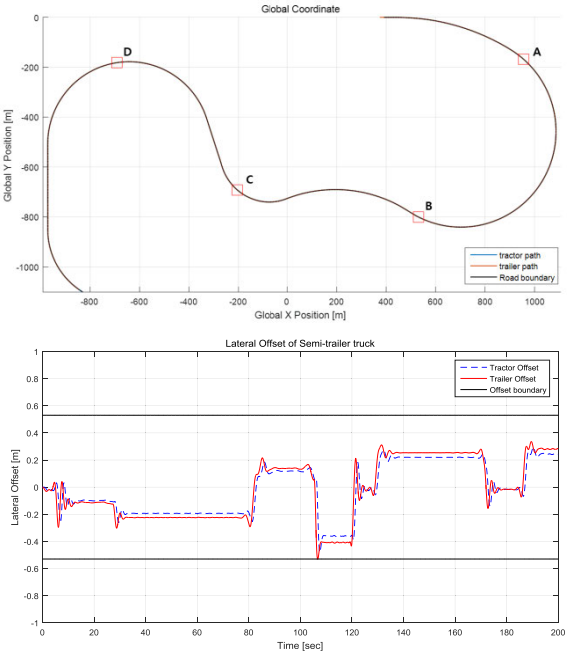


**FIGURE 22.** Result of lane keeping assist system (Global Trajectory and Lateral Offset).

## V. SIMULATION RESULTS

In order to verify the performance of the proposed control system of the semi-trailer truck, simulation was conducted by using the commercial software, MATLAB / Simulink and TruckSim. The simulation tool is constructed including vehicle state estimation, target vehicle trajectory prediction, and control algorithm. With the simulation tool, both lane keeping and collision avoidance control performance of the semi-trailer truck are evaluated.

### A. RESULT OF THE LANE KEEPING SYSTEM

In this simulation, the vehicle is driven at a constant speed of 80 km/h on the road with several corners. The road lane is 3.6m wide and the curvature of the road is designed similarly with highways. The proposed system is supposed to prevent the lane departure through the steering control intervention when the lane departure is expected.

The top plot in Figure 22 shows the trajectories of both tractor and trailer with the road boundary on the global

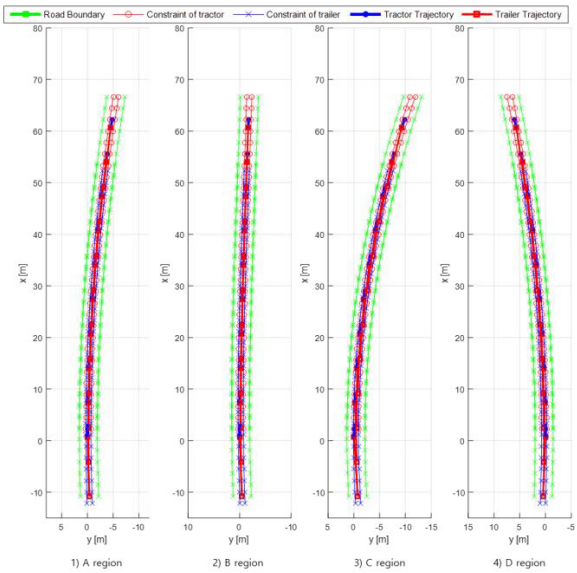


**FIGURE 23.** Result of lane keeping assist system (Local Trajectory).

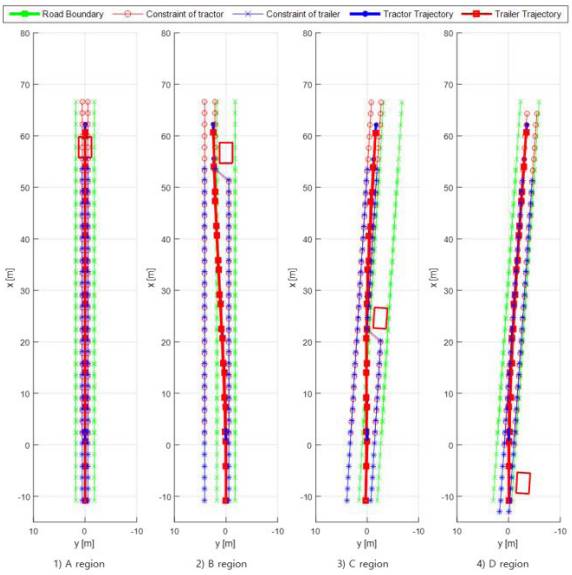


**FIGURE 25.** Lateral constraint for collision avoidance (Scenario 1).

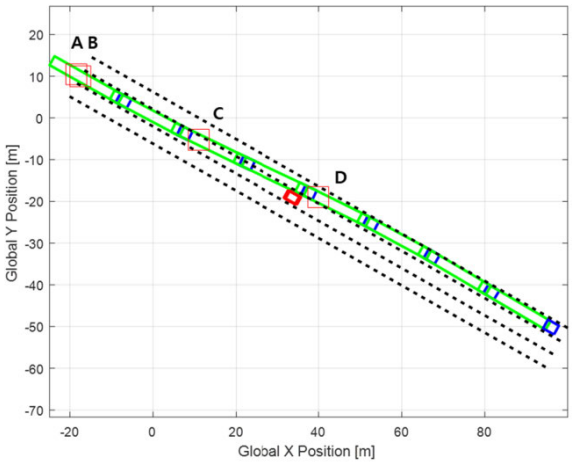


**FIGURE 24.** Result of collision avoidance maneuvering (Scenario 1).

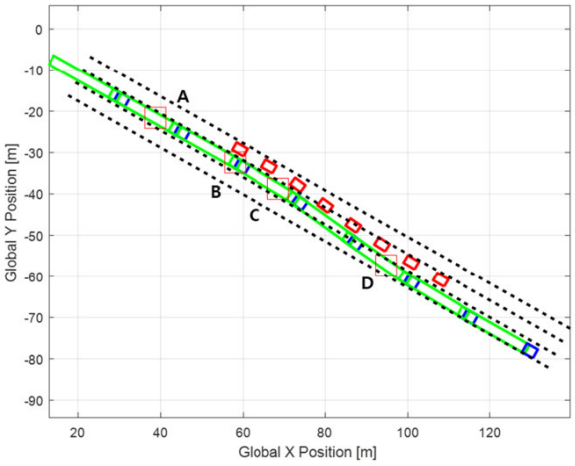


**FIGURE 26.** Result of collision avoidance maneuvering (scenario 2).

coordinate. As shown with the lateral offset at the bottom plot of Figure 22, not only the tractor, but also the trailer follows the curved road well with the proposed MPC algorithm. Four locations at point A through D in Figure 22 are amplified in Figure 23 to show road boundary, constraints for tractor and trailer and trajectories of tractor and trailer, respectively.

As shown in the plots, the proposed algorithm generates an appropriate path such that both the tractor and the semi-trailer do not deviate from the lane even on curved roads. Through these simulations, it can be confirmed that the proposed lane keeping algorithm is effective in preventing lane departure of the entire semi-trailer truck vehicle.

### *B. RESULT OF THE COLLISION AVOIDANCE SYSTEM*

Simulation is also conducted to verify the performance of the proposed collision avoidance system. The first scenario is that the semi-trailer truck drives in the middle lane at about 80 km/h, while the target vehicle at front stops in the same lane. In this situation, forward collision is expected and the semi-trailer truck steers to the left to avoid the rear-end collision.

The global trajectory of the vehicle used in the simulation is shown in Figure 24 where the entire semi-trailer truck avoids the collision. The detailed process of changing constraint is as follows. When TTC of the target vehicle is larger than the threshold, the lateral constraint of the semi-trailer truck is ego lane boundary (Figure25-1). Once the TTC of the target vehicle is smaller than the threshold, the lateral constraints at the predicted step is extended to the next lane for the collision avoidance (Figure 25-2,3,4). Using the modified lateral constraints, the proposed MPC can calculate an optimal control input for collision avoidance maneuvering.

The second scenario is that the semi-trailer truck is driving at 80 km/h, while the target vehicle on the next lane performs cut-in to the ego lane at 40 km/h. The global trajectory of

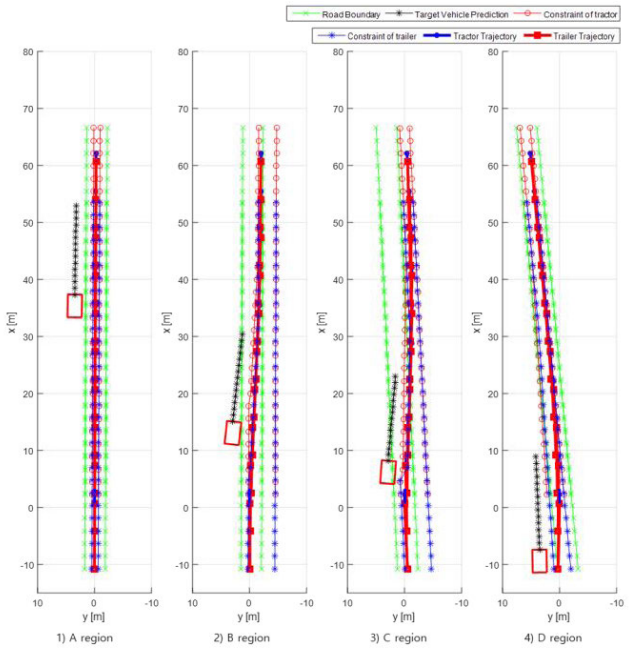


**FIGURE 27.** Lateral constraints for collision avoidance (scenario 2).

the vehicle in this simulation is shown in Figure 26 where the entire semi-trailer truck can avoid the collision even in this case. The planned local trajectory and the moving lateral constraints are illustrated in Figure 27. In Figure 27-1, even though TTC of the target vehicle is smaller than threshold, the predicted path of the target vehicle does not affect the lateral constraint of semi-trailer truck. However, when the target vehicle cuts into the ego lane, the lateral constraint is changed to generate an optimal input. The predicted path of the semi-trailer truck as well as the changed lateral constraints are shown in Figure 27-2,3,4. Using the designed constraints, the proposed MPC can calculate collision-free path in this cut-in case.

## VI. CONCLUSION

In this article, a unified lane keeping assistance and collision avoidance system is developed for a semi-trailer truck. Kinematic and dynamics models of both tractor and semi-trailer are considered first to describe the dual maneuvering paths. The accuracy of the dynamics model is largely dependent of the cornering stiffness of tires and, thus, their identification method is presented to consider their variations due to vertical load and slip angle. Because the path of semi-trailer is determined by the hitch angle which cannot be easily measured, an integrated hitch angle estimation algorithm is proposed by designing the Kalman filter based on the dynamic model and by combining with the kinematic model for the measurement update. The proposed estimation algorithm is verified in simulations and experiments with a semi-trailer truck, and their results show the accurate estimation of the hitch angle from low to high speed. By considering the lateral constraints for lane keeping and collision avoidance together, a unified Model predictive controller (MPC) is designed to calculate the desired path and the steering angle.

Constraint smoothing is suggested for the robustness of the optimal solution and model simplification with a large prediction interval is implemented for reducing the computational burden of the MPC. Finally, the proposed control system is verified in simulations with MATLAB/Simulink and TruckSim environment. The simulation results demonstrate that the proposed system is effective for lane keeping by preventing lane departure of both tractor and trailer. In addition, the proposed system shows the collision avoidance performance of the semi-trailer truck when surrounding vehicle stops or cuts-in to the ego lane.

## REFERENCES

[1] *Large Truck and Bus Crash Facts Report, Analysis Division of the Federal Motor Carrier Safety Administration*, FMCSA, Washington, DC, USA, 2016.
[2] National Highway Traffic Safety Administration (NHTSA). (2011). *Trucks in Fatal Accidents (TIFA) and Buses in Fatal Accidents (BIFA)*. Accessed: Feb. 21, 2020. [Online]. Available: https://www.nhtsa.gov/fatality-analysis-reporting-system-fars/trucks-fatal-accidents-tifa-and-buses-fatal-accidents-bifa
[3] *European Accident Research And Safety Report 2MI3*, Volvo Trucks, Gothenburg, Sweden, 2013.
[4] X. He, Y. Liu, C. Lv, X. Ji, and Y. Liu, "Emergency steering control of autonomous vehicle for collision avoidance and stabilisation," *Vehicle Syst. Dyn.*, vol. 57, no. 8, pp. 1163–1187, Aug. 2019.
[5] S. Taherian, U. Montanaro, S. Dixit, and S. Fallah, "Integrated trajectory planning and torque vectoring for autonomous emergency collision avoidance," in *Proc. IEEE Intell. Transp. Syst. Conf. (ITSC)*, Oct. 2019, pp. 2714–2721.
[6] R. Hajiloo, M. Abroshan, A. Khajepour, A. Kasaiezadeh, and S.-K. Chen, "Integrated steering and differential braking for emergency collision avoidance in autonomous vehicles," *IEEE Trans. Intell. Transp. Syst.*, early access, Apr. 13, 2020, doi: 10.1109/TITS.2020.2984210.
[7] R. Rajamani, *Vehicle Dynamics and Control*. New York, NY, USA: Springer, 2011.
[8] M. F. J. Luijten, *Lateral Dynamic Behaviour of Articulated Commercial Vehicles*. Eindhoven, The Netherlands: Eindhoven Univ. of Technology, 2010.
[9] A. V. Keller, V. A. Gorelov, D. S. Vdovin, P. A. Taranenko, and V. V. Anchukov, "Mathematical model of all-terrain truck," in *Proc. ECCOMAS Thematic Conf. Multibody Dyn.*, 2015, pp. 1285–1296.
[10] B. Simeon, F. Grupp, C. Führer, and P. Rentrop, "A nonlinear truck model and its treatment as a multibody system," *J. Comput. Appl. Math.*, vol. 50, nos. 1–3, pp. 523–532, May 1994.
[11] *Mechanical Simulation, TruckSim 8.0, Documentation and Help*, Mech. Simul. Corp., Ann Arbor, MI, USA, 2009.
[12] G. Welch and G. Bishop, *An Introduction to the Kalman Filter*. North Carolina, NC, USA: Chapel Hill, 1995.
[13] S. Li, J. Yang, W. H. Chen, and X. Chen, *Disturbance Observer-Based Control: Methods and Applications*. Boca Raton, FL, USA: CRC Press, 2014.
[14] E. F. Camacho and C. B. Alba, *Model Predictive Control*. New York, NY, USA: Springer, 2013.
[15] R. Schubert, E. Richter, and G. Wanielik, "Comparison and evaluation of advanced motion models for vehicle tracking," in *Proc. 11th Int. Conf. Inf. Fusion*, Jun. 2018, pp. 1–6.
[16] T. Zhu, X. Yin, Z. Wang, D. Wang, F. Li, X. Wang, and Z. Wang, "A novel prediction algorithm for heavy vehicles system rollover risk based on failure probability analysis and SVM empirical model," SAE Technical Paper 2020-01-0701, 2020.
[17] A. Richards, "Fast model predictive control with soft constraints," *Eur. J. Control*, vol. 25, pp. 51–59, Sep. 2015.

[18] K. Shibata, K. Nonaka, and K. Sekiguchi, "Model predictive obstacle avoidance control suppressing expectation of relative velocity against obstacles," in *Proc. IEEE Conf. Control Technol. Appl. (CCTA)*, Aug. 2019, pp. 59–64.

**JUNGGUN YANG** received the B.S. degree in mechanical engineering from Hanyang University, Seoul, South Korea, in 2014, where he is currently pursuing the Ph.D. degree with the Department of Automotive Engineering. His research interests include vehicle chassis control, autonomous driving, and driver assistance systems.

**SEUNGKI KIM** received the Ph.D. degree from Hanyang University, Seoul, South Korea, in 2017. He is currently working as a Researcher with the Research and Development Division, Hyundai Motor Company, Hwaseong, South Korea. His research interest includes vehicle chassis control based on vehicle state estimation.

**KUNSOO HUH** (Member, IEEE) received the Ph.D. degree from the University of Michigan, Ann Arbor, MI, USA, in 1992. He is currently a Professor with the Department of Automotive Engineering and the Director of the Convergence Information Technology Research Center, Hanyang University, Seoul, South Korea. His research interests include machine monitoring and control, with the emphasis on their applications to vehicular systems. His current research interests include machine fault-tolerant control, sensor-based active safety systems, vehicle-to-vehicle communication, and automated vehicle techniques.